Chalcogenide Letters Vol. 16, No. 4, April 2019, p. 143 - 148

(Co, Sm) CO-DOPED ZnS QUANTUM DOTS: MORPHOLOGICAL, STRUCTURAL, OPTICAL, PHOTOLUMINESCENCE AND PHOTOCATALYTIC PROPERTIES

M. S. PRATAP REDDY[a], P. T. POOJITHA[b], U. CHALAPATHI[c], S. V. PRABHAKAR VATTIKUTI[d], B. POORNAPRAKASH[c, *]

[a]*School of Electronics Engineering, Kyungpook National University, Daegu 41566, South Korea*

[b]*Department of Physics, Siddartha Educational Academy Group of Institutions, Tirupati 517502, India*

[c]*Department of Electronic Engineering, Yeungnam University, Gyeongsan 38541, South Korea*

[d]*School of Mechanical Engineering, Yeungnam University, Gyeongsan 38541, South Korea*

The morphological, structural, micro-structural, optical, photoluminescence, magnetic and photocatalytic properties of pure and (Co, Sm) co-doped ZnS quantum dots (QDs) fabricated via hydrothermal route are presented and distinctly discussed. X-ray diffraction (XRD) as well as the micro-Raman analysis disclosed that both pure and co-doped QDs were effectively obtained with cubic phase. The transmission electron microscopy (TEM) images divulged the fabricated QDs were monodispersed and spherical shaped. A decline in the optical bandgap was obtained in the pure ZnS QDs after (Co, Sm) co-doping. The emission of ZnS was significantly quenched via (Co, Sm) co-doping. The (Co, Sm) co-doped ZnS QDs rendered higher photocatalytic degradation of Rhodamine B (RhB) dye under artificial solar simulator irradiation than pure ZnS QDs. Thus, (Co, Sm) co-doping is a promising route to obtain the enhanced PCD of the pure ZnS QDs for photocatalysis applications.

(Received February 3, 2019; Accepted April 2, 2019)

Keywords: Zinc Sulfide; Photoluminescence; Photocatalysis.

1. Introduction

Presently, advanced routes for procuring exciting optical, electronic, photochemical, and magnetic properties of II-VI based nanocrystalline materials tempting extreme attention as anticipation for sundry applications including spintronics, optoelectronics and photocatalysis [1, 2]. Among diverse II-VI compounds, Zinc sulphide (ZnS) is an enticed material that has been explored expansively as a notable phosphor for diverse applications, due to its chemical stability, wide bandgap and large excition binding energy. Predominantly, doped nanocrystalline ZnS can enhance the optical absorption, which controls the bandgap energies, turned it suit for photocatalysis applications. Nowadays, several research groups attained the improved photocatalytic activity of ZnS even without any support of noble metal co-catalyst [3, 4]. Because of its large band gap, the theoretical efficiency of photocarrier generation of ZnS is enough higher than that of TiO_2, which may be appreciably favourable to the photocatalytic activity. Still, the efficiency of ZnS is hardly cramped by the rapid recombination of photo excited charge carriers. Moreover, due to its large band gap, which could limits its capability for solar energy harvesting. Hence, the photocatalytic activity of this material can yet be greatly improved. As is well known that, ZnS will be a promising material for photocatalytic degradation, when its bandgap is narrowed and direct recombination of charge carriers is decreased. An extensive attempts have been dedicated to either or decreasing the band gap or diminishing the recombination of photo

*Corresponding author: mail2poorna6@gmail.com

generated charge carriers of this material. Past few decades, huge convincing results have been reported on the improved photoctalytic activity of the transition or rare earth ions doped ZnS nanoparticles [5-7]. Currently, the focus shifted to the co-doped ZnS catalysts for dye degradation. In the present study, pure ZnS and (Co, Sm) co-doped ZnS QDs were prepared by hydrothermal approach.

2. Synthesis and characterizations

Pure ZnS and (Co, Sm) co-doped ZnS QDs were fabricated via the hydrothermal route. For Pure ZnS, 0.1 M of zinc acetate was dissolved in 20 mL of the double distilled water and magnetically stirred for 5 min. Next, 0.1 M of sodium sulphide solution (20 mL) was added to the above zinc solution. After that, the above product was transferred in to an autoclave and maintained at 80 °C for 180 min. After that product was rinsed with ethanol and double distilled water. Finally, heated at 60^{o}C for 15 h in an oven. Similarly, for (Co, Sm) co-doped ZnS, 0.1 M of zinc acetate, cobalt acetate (2 at%) and samarium nitrate (2 at%) were dissolved in 20 mL of the double distilled water instead of only zinc acetate and the remaining process are same as above.

The employed characterization techniques (High resolution transmission electron microscopy (HRTEM), X-ray diffraction, Raman, Diffuse reflectance spectroscopy (DRS), and Photoluminescence (PL) are the alike used in our previous articles [8, 9]. Pure ZnS and (Co, Sm)-doped ZnS QDs were calculated as catalysts for RhB dye degradation in a solution. Here, 50 mg of the catalyst were placed in a reactor with 100 ml of a solution of RhB (6 mg L^{-1}), and then, the solution was placed in the dark for 30 min to determine the adsorption-desorption of RhB on the photocatalyst surface. Finally, a simulated solar light source (300 W, Max-303 model) Xenon lamp was used. During the reaction, the samples were analyzed in a UV-Vis spectrophotometer by calculating the absorbance at 554 nm.

3. Results and discussions

3.1. TEM studies

Fig. 1 displays the the TEM and SAED (inset) patterns of the (a) pure ZnS and (b) (Co,Sm) co-doped ZnS QDs and disclose the formation of spheroid shaped particles with monodispersity. The assessed average diameter of the fabricated QDs were 7.3 and 6.6 nm for pure and (Co,Sm) co-doped ZnS QDs, respectively. From the SAED patterns, the three diffraction rings could be signed to the alike positions as the (111), (220) and (311) diffraction of bulk zinc sulfide. The absence of other diffraction rings, demonstrating that the main phase of the fabricated is cubic zinc sulfide with impure free nature.

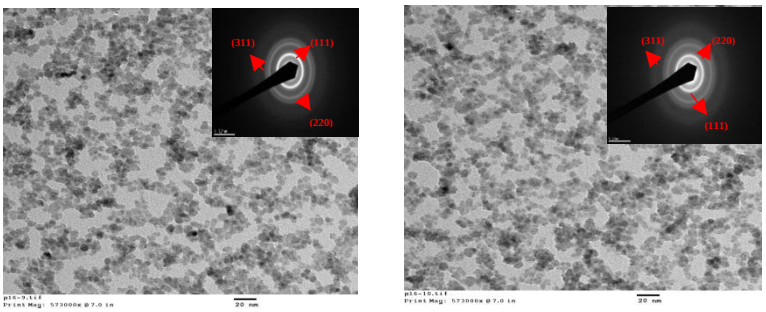

a) *b)*

Fig. 1. TEM and SAED (inset) patterns of the (a) pure and (b) (Co, Sm) co-doped ZnS QDs.

3.2. X-ray diffraction studies

To find the phase purity along with the average crystallite size of the synthesized QDs, X-ray diffraction studies were employed. The representative XRD spectra of pure and ZnS and (Co, Sm) co-doped QDs are depicted in Fig. 2 and the observed diffraction peaks could be signed to cubic phase of bulk ZnS (JCPDS Card No. 05-0566). The absence of foreign peaks suggested confirmed that the impure free nature of the fabricated QDs. The peak posture of the (Co, Sm) co-doped ZnS QDs slightly moved towards a lower 2θ value, since, the ionic radius of Sm (0.95 Å) was much bigger than that of Zn and designated the effective substitution of Co and Sm ions in the host ZnS lattice. Moreover, it is recognized that the substitution of Zn ions by Co and Sm ions diminishes the intensity of the diffraction peaks, which identically implies that the degree of crystallinity of the samples diminishes. The average crystallite size was acquired from the major (111) XRD peak using Debey-Scherrer equation, $D = 0.89\lambda/\beta \cos\theta$. The average crystallite sizes of the fabricated samples were 7.3 and 6.6 nm for the pure ZnS and (Co, Sm) co-doped ZnS QDs, respectively.

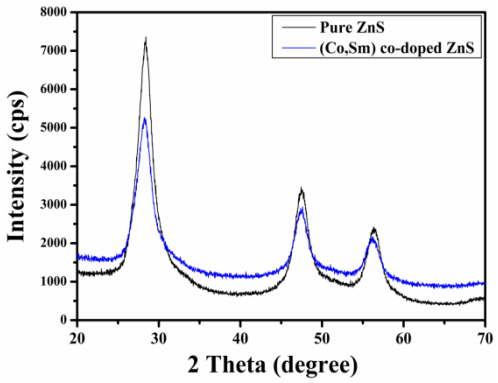

Fig. 2. XRD patterns of the pure and (Co, Sm) co-doped ZnS QDs.

3.3. Raman studies

Fig. 3 displays the micro-Raman spectra of the pure and (Co, Sm) co-doped ZnS QDs. For both QDs, the Raman modes were approximately 265 cm^{-1} and 351 cm^{-1}, which coincided with the cubic ZnS (bulk) modes [5, 8]. A petite shift of the Raman modes towards the lower frequency was recognized in the pure ZnS QDs after (Co, Sm) co-doping owing to the strain caused by the Co and Sm ions in the ZnS lattice. No extra Raman modes corresponding to any other impurities were recognized in the prepared QDs, suggesting the impure free feature of the QDs.

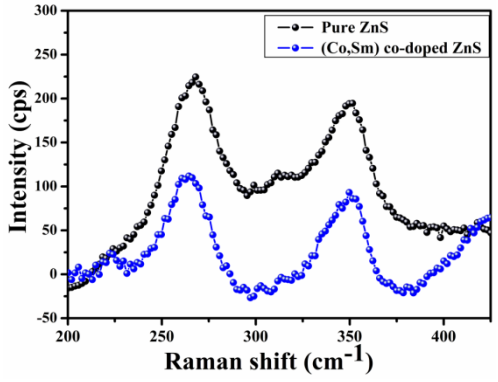

Fig. 3. Raman spectra of the pure and (Co, Sm) co-doped ZnS QDs.

3.4. DRS and PL studies

Fig. 4 (a) illustrates the DRS spectra of the pure and (Co, Sm) co-doped ZnS QDs. It is visible that, he absorption edge of the (Co, Sm) co-doped ZnS QDs was red shifted after (Co, Sm) co-doping, stipulating incorporation of the dopats as substitutes in the host lattice. The optical band gaps of the fabricated QDs were calculated from Kubelka–Munk plots, as dispalyed in Fig. 4 (b) and are 3.78 and 3.73 eV for the pure and (Co, Sm) co-doped ZnS QDs, respectively. The decreament of the bandgap is due to the sp-d or sp-f exchange interaction among the dopants and host, which is the typical phenomenon in the doped II-VI compounds [10, 11]. Fig. 6 depicts the PL spectra of the pure and (Co, Sm) co-doped ZnS QDs. All the QDs displayed alike broad emission peaks around 445 nm owing to the surface defects [12, 13]. Similar results have been reported on the similar broad emissions in the undoped and doped ZnS nanostructures [14, 15]. Although, The PL intensity of (Co, Sm) co-doped QDs dropped below that of the pure ZnS. Which is a result of co-doping and is due to repeated excitations within the Sm/Co sites and thermal escape of charge carriers from confined states to other states. Murugadoss et al. [16] also observed the enhanced fluorescence efficiency in ZnS nanoparticles through (Cu,Cd) and (Ni, Mn) co-doping. Amarantha et al. [17, 18] reported the increased PL intensity with ZnS nanoparticles via (Cu, Cr) and (Al, Mn) co-doping. No reports available on the luminescene properties of (Co, Sm) co-doped ZnS systems to compare our study with them.

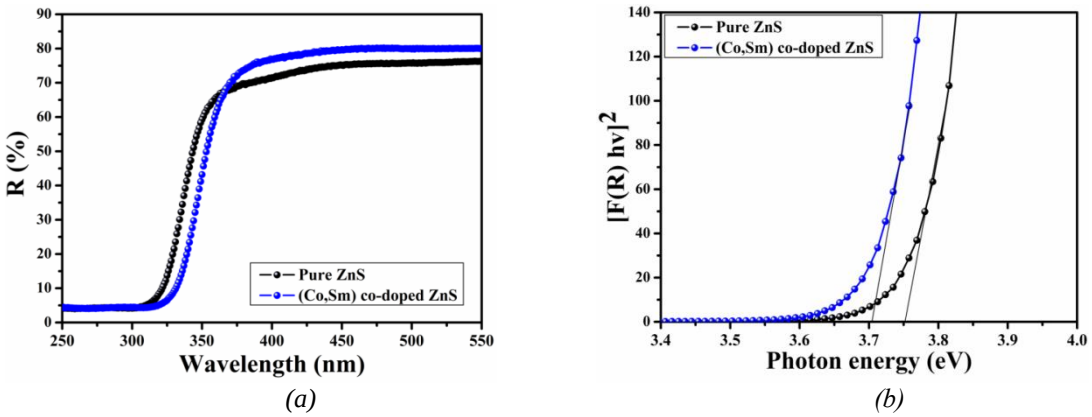

Fig. 4. (a) DRS spectra and (b) Kubelka-Munk plots of pure and (Co, Sm) co-doped ZnS QDs.

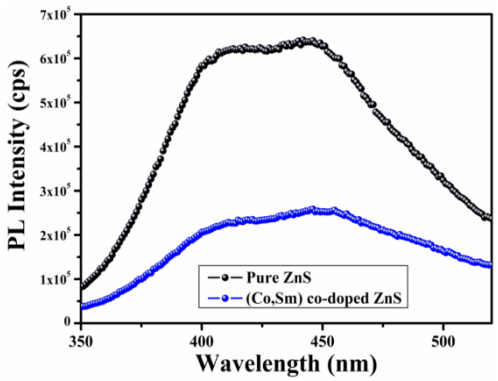

Fig. 5. PL spectra of the pure and (Co, Sm) co-doped ZnS QDs.

3.5. Photocatalysis studies

The pure and (Co, Sm)-doped ZnS QDs were utilized as sorbents for RhB B dye degradation under artificial solar simulator illumination. For 100% degradation of the RhB pollutant in an aqueous solution, 100 and 40 min were taken for pure and (Co, Sm) co-doped ZnS QDs, respectively. For a comparison, photodegradation of RhB in the dark and without a catalyst

(blank) was also performed. A graph of C/C0 verses time displayed that the (Co, Sm) co-doped ZnS QDs degraded the RhB quicker than that of the pure ZnS QDs (Fig. 6 (a)). The photocatalytic degradation (PCD) kinetics of the RhB solution with fabricated QDs under the artificial solar simulator illumination are depicted in Fig. 6 (b). The improved PCD of the (Co, Sm) co-doped ZnS QDs may be attributed to the narrowing bandgap induced by the co-doping. Moreover, the fuorescene efficiency of the (Co, Sm) co-doped ZnS QDs quenches appreciably as the co-doping upon the visible light region and manifests the decrement of the recombination of electron-hole pairs.

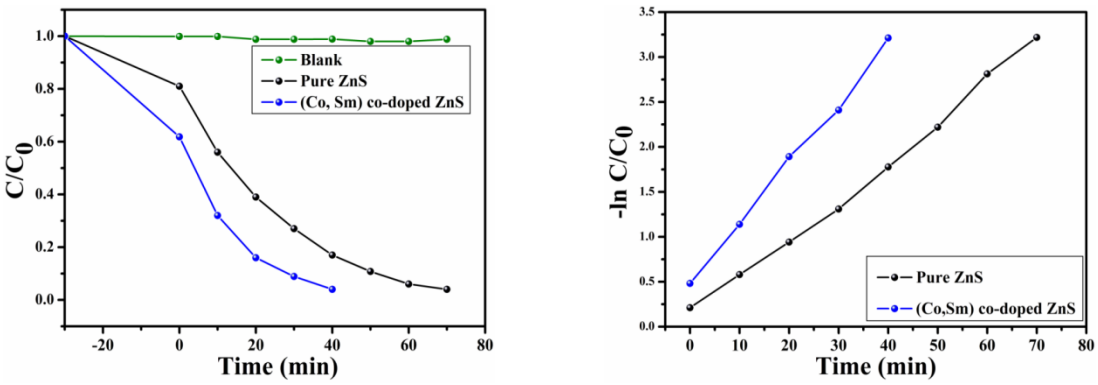

(a) (b)

Fig. 6. (a) Photocatalytic activities and (b) Kinetic linear simulations of RhB photocatalytic degradation over the pure and (Co, Sm) co-doped ZnS QDs.

4. Conclusions

In summary, pure and (Co, Sm) co-doped ZnS QDs were fabricated throug a chemical hydrothermal route. TEM images disclosed the fabricated QDs were polydispersed with spheroid shaped. XRD as well as the Raman results designated that the authentic entry of Co, Sm ions in the host lattice without changing its cubic phase. A redshift in the absorption edge was oberved in the pure ZnS after (Co, Sm) co-doping. The luminescence of pure ZnS was significantly decreased via (Co, Sm) co-doping. The higher PCD (RhB) was obtained through (Co, Sm) co-doped ZnS compared with the pure ZnS QDs catalyst. Hence, (Co, Sm) co-doping is a promising and novel approach to improve the PCD of the ZnS QDs.

Acknowledgements

This work was supported by the National Research Foundation of Korea (NRF) funded by Ministry of Education funded by the Ministry of Science, ICT and Fusion Research (2018R1D1A1B07040603) and BK21 Plus funded by the Ministry of Education (21A20131600011).

References

[1] I. V. Martynenko, A. P. Litvin, F. Purcell-Milton, A. V. Baranov, A. V. Fedorov, Y. K. Gun'ko, J. Mater. Chem. B **5**, 6701 (2017).
[2] T. Dietl, H. Ohno, Rev. Mod. Phys. **86**, 187 (2014).
[3] Yangping Hong, Jun Zhang, Xian Wang, Yongjing Wang, Zhang Lin, Jiaguo Yu, Feng Huang, Nanoscale. **4**, 2859 (2012).
[4] Jun Zhang, Jiaguo Yu, Yimin Zhang, Qin Li, Jian Ru Gong, Nano Lett. **11** (11), 4774 (2011).

[5] B. Poornaprakash, U. Chalapathi, S.V. Prabhakar Vattikuti, M. Chandra Sekhar, B. Purusottam Reddy, P. T. Poojitha, M. Siva Pratap Reddy, Youngsuk Suh, Si-Hyun Park, Ceram. Int. **45**, 2289 (2019).
[6] Philipp Weide, Katharina Schulz, Stefan Kaluza, Markus Rohe, Radim Beranek, Martin Muhler, Langmuir **32**, 12641 (2016).
[7] Gang-Juan Lee, Sambandam Anandan, Susan J. Masten, Jerry J. Wu, Renew. Energ **89**, 18 (2016).
[8] B. Poornaprakash, P. T. Poojitha, U. Chalapathi, K. Subramanyam, Si-Hyun Park, Physica E **83**, 180 (2016).
[9] B. Poornaprakash, U. Chalapathi, Maddaka Reddeppa, Si-Hyun Park, Superlattice. Microstruct. **97**, 104 (2016).
[10] B. Poornaprakash, D. Amaranatha Reddy, G. Murali, R. P. Vijayalakshmi, B. K. Reddy, Physica E **73**, 63(2015).
[11] B. Poornaprakash, S. Ramu, Si-Hyun Park, R. P. Vijayalakshmi, B. K. Reddy, Mater. Lett. **164**, 104 (2016).
[12] B. Poornaprakash, S. Sambasivam, D. Amaranatha Reddy, G. Murali, R. P. Vijayalakshmi, B. K. Reddy, Ceram. Int. **40**, 2677 (2014).
[13] B. Poornaprakash, D. Amaranatha Reddy, G. Murali, N. Madhusudhana Rao, R. P. Vijayalakshmi, B. K. Reddy, J. Alloy. Compd. **5577**, 79 (2013).
[14] N. Karar, F. Singh, B. R. Mehta, J. Appl. Phys. **95**, 656 (2004).
[15] W. Q. Peng, G. W. Cong, S. C. Qu, Z. G. Wang, Opt. Mater. **29**, 313 (2006).
[16] G. Murugadoss, J. Lumin. **132**, 2043 (2012).
[17] D. Amaranatha Reddy, G. Murali, B. Poornaprakash, R. P. Vijayalakshmi, B. K. Reddy, Appl. Surf. Sci. **258**, 5206 (2012).
[18] D. Amaranatha Reddy, Chunli Liu, R. P. Vijayalakshmi, B. K. Reddy, Ceram. Int. **40**, 1279 (2014).